Multiple elimination and transmission compensation in primary reflections in data domain

Zhang, Lele; Slob, Evert

Multiple elimination and transmission compensation in primary reflections in data domain

Lele Zhang[*]*, Evert Slob*
Delft University of Technology, 2628 CN Delft, The Netherlands

SUMMARY

We retrieve transmission compensated subsurface primary reflections from the reflection response measured at the surface. This is achieved by filtering the reflection response. The application of this scheme does not require model information. In this process, the reflection response is convolved and correlated with itself. The result after each convolution and correlation is truncated in the time domain. Free-surface and internal multiple reflections are removed and the two-way transmission effects in the primary reflections are compensated for in one step. The output of this scheme is a data set that contains only transmission compensated primary reflections. The obtained data set can be used as input to retrieve an artefact-free image of the medium. We illustrate the method with a two-dimensional example that shows how free-surface and internal multiple reflections are removed and transmission loss in primary reflections are compensated for. The method can have a wide range of applications in 3D strongly scattering media that are accessible from one side only.

INTRODUCTION

The application of reflection of acoustic or elastodynamic waves plays a central role in seismic exploration and seismology. Multiple reflection is a common phenomenon which occurs in media where velocity or density vary with position. For seismology and seismic exploration, the signal experiences multiple reflections caused by the typical heterogeneity of the Earth. The signal can be emitted by a natural, or man-made source acting on the surface and observed by receivers located kilometers away from the source. The observed signal appears as a direct arrival followed by coda waves. The multiple reflections encoded in the measured signal degrade the quality of the image (Weglein, 2016) because imaging schemes assume only primary reflections have occurred in the medium.

Several schemes have been developed to mitigate the artefacts in the image that are caused by multiple reflections. Some of them focus on removing free-surface or internal multiple reflections from measured data before the imaging procedure. Such as surface-related multiple elimination (SRME) and inverse scattering series (ISS). For SRME, the free-surface related multiple reflections can be successfully removed (Verschuur et al., 1992). For ISS, internal multiple reflections can be predicted with erroneous amplitudes and lead to partial removal (Ten Kroode, 2002; Löer et al., 2016). A revised Marchenko redatuming has been introduced recently to remove the free-surface and internal multiple

reflections in image domain with one-sided reflection response as input (Singh et al., 2015; Singh et al., 2017). Because the Marchenko redatuming creates a virtual receiver position inside the medium, it requires an estimate of the first arrival of the focusing wave field. This estimation requires a smooth velocity model to be built before the method can work. Hence, these methods either require model information in the prediction and subtraction of multiple reflections or cannot eliminate the free-surface and internal multiple reflections together.

Our aim is to find a scheme to remove free-surface and internal multiple reflections, while the amplitudes of the retrieved primary reflections are compensated for two-way transmission effects by using the measured surface reflection data as input. It is possible to separate the multiple elimination step from the imaging step in such a way that model information is only needed in the imaging step (van der Neut and Wapenaar, 2016). We present a scheme that entirely obviates the requirement of estimating the first arrival in the focusing wave field from a revised one-sided Marchenko equations (Singh et al., 2017) to eliminate free-surface and internal multiple reflections and compensate for transmission loss in primary reflections in one step. One-sided reflection data is required as input and no model information is needed. Because multiple reflections are eliminated, the retrieved data set contains only primary reflections. The compensation for transmission effects enhances the amplitude of the retrieved primary reflection data. We then argue that the result of our method is more convenient to perform seismic migration to obtain a subsurface image with high amplitude fidelity. The retrieved primary reflections can be used in standard velocity model estimation and amplitude versus offset analysis as well. Once the velocity model is found the data set can be used to create an artefact-free image using standard imaging techniques.

THEORY

We indicate time as t and the position vector of a spatial location as $\mathbf{x} = (x, y, z)$, where z denotes depth and (x, y) denote the horizontal coordinates. The free surface $\partial \mathbf{D}_0$ is defined for all (x, y) at $z_0 = 0$. For convenience, the coordinates at $\partial \mathbf{D}_0$ are denoted as $\mathbf{x}_0 = (\mathbf{x}_H, z_0)$, with $\mathbf{x}_H = (x, y)$. Similarly, the position vector of a point at an arbitrary depth level $\partial \mathbf{D}_i$ is denoted as $\mathbf{x}_i = (\mathbf{x}_H, z_i)$, where z_i denotes the depth of $\partial \mathbf{D}_i$. We express the

acoustic impulse reflection response as $R(\mathbf{x}_0', \mathbf{x}_0, t)$, where $\mathbf{x}_0$ denotes the source position and $\mathbf{x}_0'$ denotes the receiver position, both located at the free surface $\partial\mathbf{D}_0$. The focusing wave field $f_1(\mathbf{x}_0, \mathbf{x}_i, t)$ is the solution of the homogeneous wave equation in a truncated medium and focuses at the focal point $\mathbf{x}_i$. We define the truncated domain as (x, y) in R and $z_0 < z < z_i$. Inside the truncated domain, the properties of the medium are equal to the properties of the physical medium. Outside the truncated domain, the truncated medium is reflection-free. The Green's function $G(\mathbf{x}_i, \mathbf{x}_0, t)$ is defined for an impulsive source that is excited at $\mathbf{x}_0$ and a receiver is positioned at the focal point $\mathbf{x}_i$. The Green's function is defined in the same physical medium as the measured data. The focusing and Green's functions can be partitioned into up- and downgoing constituents and for this we use pressure-normalized quantities.

We start with the 3D versions of one-way reciprocity theorems for pressure-normalized wave fields and use them for the depth levels z_0 and z_i. Because of the presence of a free surface at the acquisition level z_0, the Green's function representations are given by (Singh et al., 2017),

$$G^-(\mathbf{x}_i, \mathbf{x}_0', t) = \int_{\partial\mathbf{D}_0} d\mathbf{x}_0 \int_0^{+\infty} [R(\mathbf{x}_0', \mathbf{x}_0, t') f_1^+(\mathbf{x}_0, \mathbf{x}_i, t - t')$$
$$- rR(\mathbf{x}_0', \mathbf{x}_0, t') f_1^-(\mathbf{x}_0, \mathbf{x}_i, t - t')]dt' \qquad (1)$$
$$- f_1^-(\mathbf{x}_0', \mathbf{x}_i, t),$$

$$G^+(\mathbf{x}_i, \mathbf{x}_0', -t) = -\int_{\partial\mathbf{D}_0} d\mathbf{x}_0 \int_{-\infty}^0 [R(\mathbf{x}_0', \mathbf{x}_0, -t') f_1^-(\mathbf{x}_0, \mathbf{x}_i, t - t')$$
$$- rR(\mathbf{x}_0', \mathbf{x}_0, -t') f_1^+(\mathbf{x}_0, \mathbf{x}_i, t - t')]dt'$$
$$+ f_1^+(\mathbf{x}_0', \mathbf{x}_i, t).$$
$$(2)$$

Superscripts $+$ and $-$ stand for downgoing and upgoing fields, respectively. The r indicates the reflection coefficient of the free surface. The downgoing component of the focusing function $f_1^+(\mathbf{x}_0, \mathbf{x}_i, t)$ is the inverse of the transmission response in the truncated medium (Wapenaar et al., 2013). We can write both the focusing function and the transmission response as the sum of a direct part and a coda

$$f_1^+(\mathbf{x}_0, \mathbf{x}_i, t) = f_{1d}^+(\mathbf{x}_0, \mathbf{x}_i, t) + f_{1m}^+(\mathbf{x}_0, \mathbf{x}_i, t), \qquad (3)$$

$$T(\mathbf{x}_i, \mathbf{x}_0, t) = T_d(\mathbf{x}_i, \mathbf{x}_0, t) + T_m(\mathbf{x}_i, \mathbf{x}_0, t), \qquad (4)$$

where f_{1d}^+ and T_d indicate the direct part, whereas f_{1m}^+ and T_m indicate the following coda. Because the Green's and focusing functions in equations 1 and 2 are separated in time domain except for one time instant, we can rewrite equations 1 and 2 with the help of equation 3 as

$$f_1^-(\mathbf{x}_0', \mathbf{x}_i, t) = \int_{\partial\mathbf{D}_0} d\mathbf{x}_0 \int_0^{+\infty} [R(\mathbf{x}_0', \mathbf{x}_0, t') f_1^+(\mathbf{x}_0, \mathbf{x}_i, t - t')$$
$$- rR(\mathbf{x}_0', \mathbf{x}_0, t') f_1^-(\mathbf{x}_0, \mathbf{x}_i, t - t')]dt',$$
$$\text{for } -t_d + \varepsilon < t < t_d + \varepsilon \quad (5)$$

$$f_{1m}^+(\mathbf{x}_0', \mathbf{x}_i, t) = \int_{\partial\mathbf{D}_0} d\mathbf{x}_0 \int_{-\infty}^0 [R(\mathbf{x}_0', \mathbf{x}_0, -t') f_1^-(\mathbf{x}_0, \mathbf{x}_i, t - t')$$
$$- rR(\mathbf{x}_0', \mathbf{x}_0, -t') f_1^+(\mathbf{x}_0, \mathbf{x}_i, t - t')]dt',$$
$$\text{for } -t_d + \varepsilon < t < t_d + \varepsilon \quad (6)$$

where t_d denotes the one-way travel time from the surface point $\mathbf{x}_0'$ to the focusing point $\mathbf{x}_i$, and ε is a positive value to account for the finite bandwidth. Note that the time truncation operator in equations 5 and 6 is asymmetric and different than used in the standard Marchenko scheme. Wapenaar et al. (2014) show that

$$\int_{\partial\mathbf{D}_i} d\mathbf{x}_i \int_0^{+\infty} T_d(\mathbf{x}_i, \mathbf{x}_0'', t') f_{1d}^+(\mathbf{x}_0, \mathbf{x}_i, t - t')dt' = \delta(\mathbf{x}_H'' - \mathbf{x}_H)\delta(t),$$
$$(7)$$

where $\delta(\mathbf{x}_H)$ is a spatially band-limited 2D delta function in space and $\delta(t)$ is a delta function in time. Equation 7 shows that T_d is the inverse of f_{1d}^+. Following van der Neut and Wapenaar (2016), we apply this convolution integral operator to equations 5 and 6 to find

$$v^-(\mathbf{x}_0', \mathbf{x}_0'', t) =$$
$$\int_{\partial\mathbf{D}_0} d\mathbf{x}_0 \int_0^{+\infty} [R(\mathbf{x}_0', \mathbf{x}_0, t')(\delta(t - t')\delta(\mathbf{x}_H'' - \mathbf{x}_H)$$
$$+ v_m^+(\mathbf{x}_0, \mathbf{x}_0'', t - t')) - rR(\mathbf{x}_0', \mathbf{x}_0, t')v^-(\mathbf{x}_0, \mathbf{x}_0'', t - t')]dt',$$
$$\text{for } \varepsilon < t < t_2 + \varepsilon \quad (8)$$

$$v_m^+(\mathbf{x}_0', \mathbf{x}_0'', t) =$$
$$\int_{\partial\mathbf{D}_0} d\mathbf{x}_0 \int_{-\infty}^0 [R(\mathbf{x}_0', \mathbf{x}_0, -t')v^-(\mathbf{x}_0, \mathbf{x}_0'', t - t')$$
$$- rR(\mathbf{x}_0', \mathbf{x}_0, -t')(\delta(t - t')\delta(\mathbf{x}_H'' - \mathbf{x}_H) + v_m^+(\mathbf{x}_0, \mathbf{x}_0'', t - t'))]dt',$$
$$\text{for } \varepsilon < t < t_2 + \varepsilon \quad (9)$$

where v^- and v_m^+ are convolved versions of f_1^- and f_{1m}^+ as is shown in equation 7 for f_{1d}^+, t_2 denotes the two-way travel time from a surface point $\mathbf{x}_0'$ to the focusing level z_i and back to the surface point $\mathbf{x}_0''$. These two equations can be seen as the projected version of the revised couple-Marchenko equations that take free-surface multiple reflections into account. The focusing functions can be obtained by using the delta function as initial input showing that the scheme is model-free now. The t_2 in equations 8 and 9 is the two-way travel time from the surface to the depth level in the subsurface where we have focused to and projected back from. When the focusing level coincides with an actual subsurface reflector, the last event in v^- at

time instant t_2 will be the transmission loss compensated primary reflection of that reflector with two-way travel time t_2. The reason is that v^- is the convolved version of f_1^- and the final event in f_1^- is the response to f_{1d}^+ of that reflector (note that f_{1d}^+ is the inverse of T_d). Otherwise, the value in v^- at time instant t_2 will be zero. This means that v^- can be evaluated and its last event can be picked to represent a possible primary reflection event of the medium without transmission losses. Because we do not have to specify the focusing level the time instant t_2 can be chosen as t and we extract the value of v^- for each value of t and store it in a new function containing only the transmission loss compensated subsurface primary reflections. We can write it as

$$R_r(\mathbf{x}_0'',\mathbf{x}_0',t) = v^-(\mathbf{x}_0'',\mathbf{x}_0',t). \tag{10}$$

where R_r denotes the retrieved primary reflections whose amplitudes are compensated for two-way transmission effects.

Equations 8 and 9 can be evaluated to obtain the transmission loss compensated primary reflections that are stored in a new data set in equation 10. Note that the free-surface and internal multiple reflections are removed and that the transmission effects in the primary reflections are compensated for in one step. The retrieved data set is more suitable for velocity model estimation and standard imaging than the original data. Moreover, we can see the scheme as a mechanism to determine which parts of the data are predictable from the parts that are not. The non-predictable parts are retained in this expression. These include the primary reflections, refracted waves and forward scattered waves (these non-primary reflections will be treated as primary reflections by our scheme and related artefacts will be created after the processing). The predictable parts are removed from this expression. These include the free-surface and internal multiple reflections and transmission losses in primary reflections. The processing can be performed without any model information.

EXAMPLE

The aim of the current method is to retrieve the primary reflections by removing the free-surface and internal multiple reflections and to compensate for transmission effects in the primary reflections given the measured reflection response at one side of the medium as input. A 2D numerical example is given to illustrate the method. Figure 1(a) shows the values for the acoustic velocity as a function of depth and horizontal positions, Figure 1(b) gives the values for the density of the medium as a function of depth and horizontal positions. The source emits a

Ricker wavelet with $20\,\text{Hz}$ centre frequency. Absorbing boundary conditions are applied at two sides and bottom of the model, the top boundary of the model is set as free surface (the reflection coefficient of this free surface is -1). We have computed the single-sided reflection responses with 601 sources and 601 receivers with a spacing of $10\,\text{m}$ at the free-surface boundary. One of the computed single-sided reflection responses $\widehat{R}(\mathbf{x}_0',\mathbf{x}_0'',t)$ (the hat indicates the quantity has been convolved with the source wavelet) is shown in Figure 2(a). Note that free-surface and internal multiple reflections occur at later times and the later arriving primary reflections are relatively weak because of the transmission losses. This reflection response is used as input to solve equations 8 and 9 for v^- corresponding to different focusing depth levels. Then the procedure as described using equation 10 leads to the retrieved transmission loss compensated primary reflections $\widehat{R}_r(\mathbf{x}_0'',\mathbf{x}_0',t)$ as shown in Figure 2(b). Note that free-surface and internal multiple reflections visible in Figure 2(a) have disappeared, whereas the last two primary reflection events, which cannot be distinguished from multiple reflections in Figure 2(a), are clearly retrieved in Figure 2(b). We pick the zero-offset traces from the data sets shown in Figures 2(a) and (b) and show them in Figure 3. It can be seen that free-surface and internal multiple reflections have been successfully removed and transmission losses in primary reflections have been well compensated after the processing. The red dotted line (RET) indicates the trace from the retrieved data set with higher amplitude because of the compensation for transmission effects. Both traces have been normalised by the same normalization factor.

In the derivation of the current method, we assumed a lossless medium. The method can be adapted to work with two-sided reflection and transmission data in dissipative media (Slob, 2016). We further assumed that the Green's and focusing functions can be separated in time, that the source wavelet can be well recovered and we ignored evanescent waves (Wapenaar et al., 2013). These restrictions limit the application of the current method, but not more than existing methods that require model information before the free-surface and internal multiple reflections are removed and transmission losses are compensated for. For situations in which these assumptions are fulfilled, the current method would have a nearly perfect performance as is shown with the 2D numerical example.

CONCLUSIONS

We have shown that the one-sided reflection response can be used as a filter to retrieve the transmission loss compensated primary reflections and remove free-surface

and internal multiple reflections contained in itself. No model information is required and the intermediate time window is applied after each convolution or correlation. The 2D numerical example shows that the method effectively removes free-surface and internal multiple reflections and compensates for transmission loss contained in primary reflections in one step. We expect that the current method can be used in seismological reflection imaging and monitoring of structures and processes in the Earth's interior. In all of these applications, the material under investigation needs to be accessible only from one side.

ACKNOWLEDGMENTS
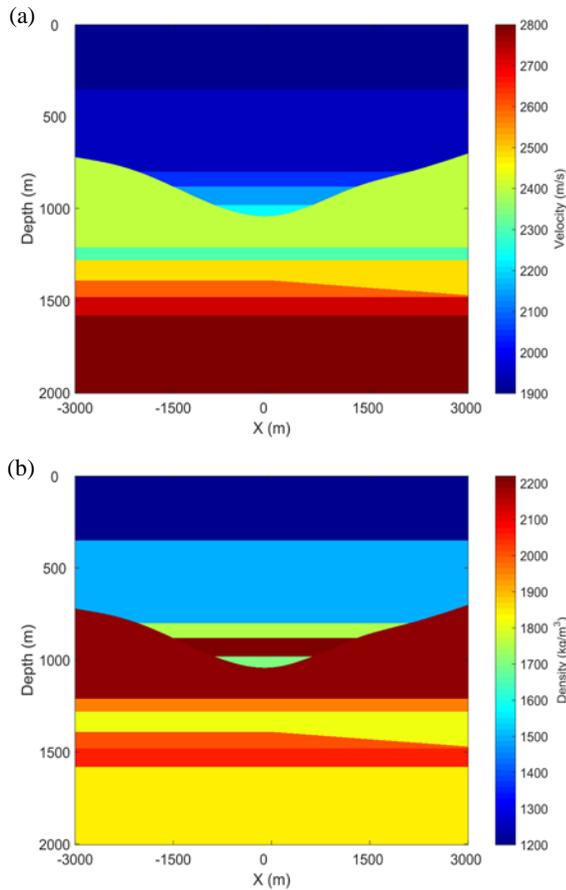
Figure 1: (a) Acoustic velocity and (b) density of the medium.
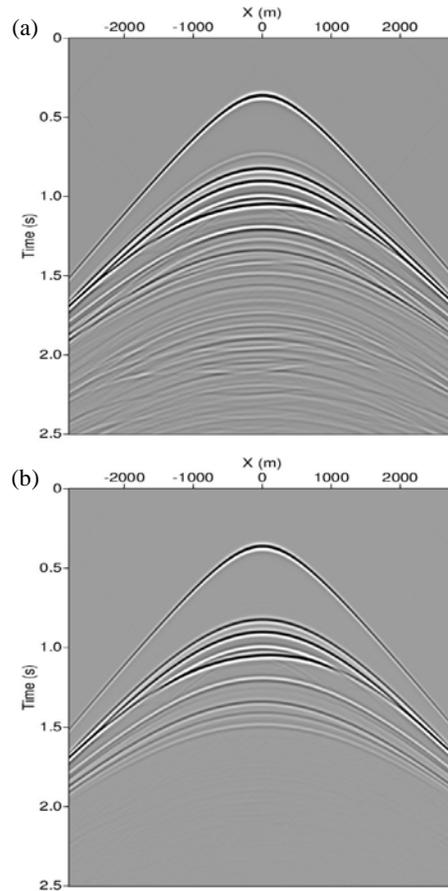
Figure 2: (a) The modeled reflection response and (b) the retrieved transmission compensated primary reflections using equation 10.
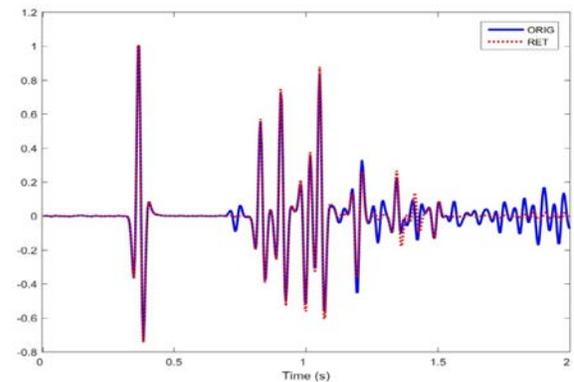
Figure 3: The comparison of zero-offset traces, the blue solid line (ORIG) comes from the original shot gather shown in Figure 2(a) and the red dotted line (RET) comes from the retrieved transmission loss compensated primary reflections shown in Figure 2(b).